

# Combined Wide-Field Imaging in Grading Diabetic Retinopathy

**Matteo Menean**

**Riccardo Sacconi**

**Beatrice Tombolini**

Department of Ophthalmology of San Raffaele Scientific Institute (Milan, Italy)

**Fantaguzzi Federico**

**Francesco Bandello**

Scientific Institute San Raffaele, Vita-Salute University - Milan

**Giuseppe Querques** (✉ [giuseppe.querques@hotmail.it](mailto:giuseppe.querques@hotmail.it))

University Vita-Salute, IRCCS San Raffaele <https://orcid.org/0000-0002-3292-9581>

---

## Article

**Keywords:** diabetic retinopathy, neovascularization, intraretinal microvascular abnormalities, colour fundus photography, OCT-Angiography

**Posted Date:** November 30th, 2022

**DOI:** <https://doi.org/10.21203/rs.3.rs-2210134/v1>

**License:**   This work is licensed under a Creative Commons Attribution 4.0 International License.

[Read Full License](#)

---

**Version of Record:** A version of this preprint was published at Eye on July 31st, 2023. See the published version at <https://doi.org/10.1038/s41433-023-02666-x>.

# Abstract

**Objectives:** To detect retinal neovascularization elsewhere (NVE), of the optic disc (NVD) and intraretinal microvascular abnormalities (IRMA) in treatment naïve diabetic retinopathy (DR) and compare these findings by using 90° Wide-Field Color Fundus Photography (WF CFP), Wide-Field Spectral-Domain Optical Coherence Tomography Angiography (OCTA) and the combination of WF CFP and OCTA through overlay software.

**Methods:** Patients with treatment naïve severe non-proliferative DR or proliferative DR were prospectively enrolled. All patients underwent WF-CFP and OCTA in the same day. Two readers independently analysed WF-CFP, SD-OCTA and the overlay of the two techniques. The degree of agreement between the two raters and between different techniques (WF CFP, OCTA, WF CFP combined to OCTA) were measured with Cohen's Kappa coefficient.

**Results:** Thirty-one eyes from 21 patients (10 males, mean age  $63 \pm 15$  years) were included. Inter-rater agreement by using WF-CFP in detection of NVE, NVD and IRMA was respectively 0.62, 0.22 and 0.55. OCTA scored values of inter-rater agreement of 0.86, 0.87 and 0.92 in detection of NVE, NVD and IRMA, respectively. By combining WF-CFP and SD-OCTA, inter-rater agreement in detection of NVE, NVD and IRMA was 0.93, 0.94 and 0.89, respectively.

**Conclusion:** Inter-rater agreement in detection of NVE, NVD and IRMA was substantial, fair and moderate, respectively. OCTA provided almost perfect values of inter-rater agreement in NVE, NVD and IRMA detection. Combining WF-CFP and OCTA further empowered concordance values in detection of NVE and NVD. Combining OCTA and WF-CFP is the best performance to detect NVE and NVD.

## Introduction

Early detection and treatment of different grades of diabetic retinopathy (DR) are widely recognized as fundamental goals to reduce visual impairment in patients with diabetes.<sup>1,2</sup> Consequently, a standardized and systematic classification for severity grading of DR is essential for therapeutic decisional process. According to the Early Treatment Diabetic Retinopathy Study (ETDRS) findings and the International Clinical Disease Severity Scale for DR, severity grading is univocally established based on color fundus photography (CFP) and direct fundus examination.<sup>3</sup> Although this international DR scale is widely recognized and simple to use in common clinical practice, there is an increasing need to implement fundus findings with multimodal imaging examinations for therapeutic decision-making and DR severity grading.<sup>4-6</sup>

Among the landscape of lesions and findings of diabetic retinopathy, intraretinal microvascular abnormalities (IRMA) showed a fair inter-rater agreement at color fundus photography.<sup>7</sup> The complete agreement in IRMA detection between two independent ophthalmologists has been assessed at 51.5% (weighted kappa statistics = 0.49).<sup>7</sup> Concurrently, the agreement in the detection at CFP of retinal

neovascularization elsewhere (NVE) was considered as substantial, while the agreement in the detection of retinal neovascularization of the optic disc (NVD) yielded less satisfactory results and has been ranked as moderate (weighted kappa statistics = 0.48).<sup>7</sup>

As the severity of IRMA and retinal neovascularization is considered by ETDRS as an important factor for photocoagulation treatment strategy choice, it is fundamental to supplement these findings with multimodal imaging techniques.<sup>8</sup> Particularly, spectral domain optical coherence tomography angiography (SD-OCTA) showed a higher detection rate of IRMA, compared to color fundus photography grading. In addition, structural spectral-domain optical coherence tomography (SD-OCT) allowed to a better characterization and differentiation of IRMA and NVE.<sup>9</sup>

An overlay between CFP and angiographic data (SD-OCTA) allows a more comprehensive analysis of the landscape of pathological findings in DR. Matching anatomical (CFP) and functional (SD-OCTA) data could improve both the detection rate and the inter-rater agreement of IRMA and retinal neovascularization indeed.

Purpose of the study is to detect intraretinal microvascular abnormalities, retinal neovascularization elsewhere and retinal neovascularization of the optic disc in treatment naïve diabetic retinopathy and to compare these findings by using 90° Wide-Field Color Fundus Photography (WF-CFP), Wide-Field Spectral-Domain Optical Coherence Tomography Angiography (UWF SD-OCTA) and the combination of WF-CFP and UWF SD-OCTA through overlay software.

## Methods

This was a prospective observational monocentric study of patients affected by treatment naïve diabetic retinopathy enrolled at the Retina Medica and Imaging Unit of Department of Ophthalmology of San Raffaele Scientific Institute, Milan (Italy) from September 2021 to February 2022. This study was conducted under the tenets of the Declaration of Helsinki (1964). Written patients' informed consent was obtained.

We included eyes with severe non-proliferative diabetic retinopathy (SNPDR) or proliferative diabetic retinopathy (PDR), according to the International Clinical Diabetic Retinopathy and Diabetic Macular Edema Disease Severity Scales.<sup>3</sup> Both patients with type 1 and type 2 diabetes mellitus were enrolled in the study. Exclusion criteria were prior laser or intravitreal treatments in the included eye, any retinal disease than diabetic retinopathy, DR related complications impeding retinal imaging (vitreous haemorrhage, retinal detachment, corneal oedema) and optic media opacities limiting image quality.

We collected age, gender, medical and ocular history. Each included eye underwent WF-CFP centred on the fovea and SD-OCTA, with a scan field of 12x12 mm<sup>2</sup> centred on the fovea.

WF-CFP was performed with Clarus® (ZEISS, Oberkochen, Germany). At fundus color photography, we defined NVE as neovascularization that are on the surface of the retina or further forward in the vitreous

cavity, except for those on the disc or within 1 optic disc diameter of its margin.<sup>7</sup> (Figure 1A) Conversely, a neovascularization that fulfil the abovementioned criteria, located on the optic disc or within 1 optic disc diameter, was indicated as NVD. (Figure 2A) IRMA were defined as tortuous intraretinal vascular segments of variable diameter (within ¼ the width of a major vein at the disc margin).<sup>7</sup> (Figure 3A)

SD-OCTA was performed with Cirrus 6000® (ZEISS, Oberkochen, Germany) and examined with Angioplex® OCTA software (ver. 11.5.2, ZEISS, Oberkochen, Germany). SD-OCTA slabs were automatically segmented by SD-OCTA software and independently manually adjusted by two ophthalmologists (MM and RS). Vitreoretinal interface (VRI) slab, defined as the region 10 to 300 µm above the internal limiting membrane (ILM), was selected to detect NVE and NVD (Figure 1B; Figure 2B). Each suspected neovascularization was confirmed at B-scan as extraretinal proliferation. Superficial capillary plexus (SCP) slab was defined as the region between the inner nuclear layer (INL) and the ILM and selected to detect IRMA, identified as dilated terminal vessels adjacent to areas of capillary loss.<sup>10</sup> (Figure 3B)

Both VRI and SCP slabs were combined to WF-CFP through the overlay software (ZEISS Forum Viewer®, Carl Zeiss Meditec, Inc, Dublin, California, Usa) to detect NVE, NVD and IRMA. (Figure 1C; Figure 2C; Figure 3C)

Two readers expert in medical retina (MM and BT) independently analysed WF-CFP, SD-OCTA and the overlay of the two techniques to detect and record the number and location of NVE, NVD and IRMA. Statistical analyses were performed using SPSS Statistics Software version 27.0 (IBM, Armonk, New York, USA). We summarized continuous variables as their mean ± standard deviation (SD). We summarized categorical variables as their absolute and relative prevalence. The degree of agreement in detecting NVE, NV and IRMA between the two readers and between different imaging techniques (WF CFP, UWF SD-OCTA, WF CFP combined to UWF SD-OCTA) were measured with Cohen's Kappa (k) coefficient. Cohen's Kappa (k) values were interpreted as slight when between 0.00 and 0.20, as fair when 0.21-0.40, as moderate when 0.41-0.60, as substantial when 0.61-0.80. Cohen's Kappa (k) values indicated almost perfect agreement when 0.81-1.00, while values <0.00 disclosed no agreement.<sup>11</sup>

## Results

Thirty-one eyes from 21 patients were included in the study. Patients' mean age was 63 ± 15 years. Ten (48%) out of 21 patients were male. Best-corrected visual acuity was 6/12 Snellen Equivalent (IQR 6/6-6/15). Two eyes (6.5%) presented with severe proliferative diabetic retinopathy, 21 eyes (67.7%) were affected by proliferative diabetic retinopathy and 8 eyes (25.8%) by severe non-proliferative diabetic retinopathy. Demographic and clinical features of patients enrolled were reported in Table 1.

Inter-rater agreement by using WF-CFP in detection of NVE, (Figure 1.A) NVD (Figure 2.A) and IRMA (Figure 3.A) was respectively 0.62, 0.22 and 0.55. SD-OCTA disclosed values of inter-rater agreement of 0.86, 0.87 and 0.92 in detection of NVE, (Figure 1.B) NVD (Figure 2.B) and IRMA, (Figure 3B), respectively.

By combining WF-CFP and SD-OCTA through overlay software, inter-rater agreement in detection of NVE, (Figure 1.C) NVD (Figure 2.C) and IRMA (Figure 3.C) was 0.93, 0.94 and 0.89, respectively.

WF-CFP and SD-OCTA showed concordance values of 0.15, 0.26 and 0.17 in detection of NVE, NVD and IRMA, respectively. In detection of NVE, NVD and IRMA, combination of WF-CFP and SD-OCTA through overlay software compared to CFP scored concordance values of 0.35, 0.13 and 0.17, respectively. Combination of WF-CFP and SD-OCTA through overlay software compared to SD-OCTA showed concordance values of 0.59, 0.74 and 0.57, in detection of NVE, NVD and IRMA, respectively. Inter-rater agreement between readers and concordance between techniques were summarized in Table 2A and 2B, respectively.

## Discussion

Grading DR is an essential step for therapeutic decisional process.<sup>1</sup> Determining the presence of neovascularization and IRMA is still a challenge, since inter-rater agreement values in detection of these lesions do not provide adequate results.<sup>7</sup> OCTA could contribute in better characterization and detection of IRMA and neovascularization. We investigated whether combining anatomical data from WF-CFP and functional flow data from OCTA could improve the rate and the inter-rater agreement in detection of IRMA, NVE and NVD.

We found substantial (0.62), fair (0.22) and moderate (0.55) inter-rater agreement at WF-CFP in detection of NVE, NVD and IRMA, respectively. OCTA provided better values of inter-rater agreement. Particularly, Cohen's kappa significantly improved in NVD detection, displaying almost perfect inter-rater agreement (0.87), as well as in NVE (0.86) and IRMA (0.92) detection. Combining WF-CFP and OCTA through overlay software further empowered concordance values in detection of NVE (0.93) and NVD (0.94), while concordance values in IRMA detection were slightly lower compared to OCTA but almost perfect (0.89).

WF-CFP and OCTA scored slight (0.26) and fair (0.15, 0.17) concordance values in detection of NVD, NVE and IRMA, respectively. Concordance values between WF-CFP and WF-CFP combined to OCTA were poor, as well. However, OCTA and WF-CFP combined to OCTA scored moderate (0.59, 0.57) or substantial (0.74) values in detection of NVE, IRMA and NVD respectively.

Distinguishing neovascularization from other findings related to DR represents a challenge for non-retina specialists.<sup>12</sup> Vascular abnormalities or haemorrhages are often confused with neovascularization, and concurrently neovascularization is thin, slightly coloured and is frequently missed when examined from a non-retina specialist ophthalmologist. Particularly, NVD detection could represent a challenge due to the underlying vascular network in the optic disc and explain the low value of inter-rater agreement at WF-CFP.<sup>13</sup> A-scan and B-scan OCTA helps in detection of NVE and NVD; ophthalmologists are able to localize whether the lesion is inside the vitreoretinal interface or not, distinguishing neovascularization from IRMA, and to characterize the presence of flow inside the abovementioned lesions. In our experience, this tool has improved inter-rater agreement in detection of both NVE and NVD. On the other hand, OCTA alone

does not provide anatomical data and wrong segmented layer or artefacts could lead to misinterpreted data. Combining OCTA and WF-CFP with the overlay software allows better characterization of the lesions, since complementary data are merged, flow signal at B-scan can be analysed in the counterpart WF-CFP, and artefacts or wrong segmented layers can be better highlighted. As a matter of fact, WF-CFP combined with OCTA provided better values of inter-rater agreement in NVE and NVD detection.

IRMA detection at WF-CFP disclosed poor inter-rater agreement (0.22). Since IRMA appear as abnormal branching or dilation of existing blood vessels in low-blood supply retinal area, they can be often confused with neovascularization or misinterpreted. OCTA highlights their tortuosity and their location in non-perfusion areas, and most importantly they can be easily distinguished from neovascularization, since IRMA localize in the superficial capillary plexus.<sup>14</sup> According to our results, the combination of OCTA and WF-CFP did not improve inter-rater agreement.

The main limitation of the study is the relatively small sample size. In addition, inter-rater agreement of the considered imaging techniques could have been explored between ophthalmologists of different level of experience. Indeed, young ophthalmologists could eventually benefit the most from combining OCTA and WF-CFP.

In conclusion, combining OCTA and WF-CFP displayed good concordance values in detection of NVD and NVE, compared to OCTA. In addition, the overlay between the two techniques has shown better concordance values, particularly in NVE and NVD detection, as previously discussed. Thus, this tool could help ophthalmologists improving detection of clinical findings of diabetic retinopathy, particularly NVD and NVE. Further studies are required to confirm whether combining OCTA and WF-CFP could help detecting other findings (i.e. microaneurysms), and whether even retina specialists could improve their skills.

## **Declarations**

### **Author Disclosure Statement**

MM, BT, FF have nothing to disclose. RS has the following disclosures: Allergan Inc, Bayer Shering-Pharma, Medivis, Novartis, Zeiss.

FB has the following disclosures: Allergan Inc, Bayer Shering-Pharma, Boehringer-Ingelheim, Fidia Sooft, Hofmann La Roche, Novartis, NTC Pharma, Oxurion NV, Sifi.

GQ has the following disclosures: Alimera Sciences, Allergan Inc, Amgen, Bayer Shering-Pharma, Heidelberg, KBH, LEH Pharma, Lumithera, Novartis, Sandoz, Sifi, Sooft-Fidea, Zeiss

### **Acknowledgements**

Funding/Support: This research did not receive any specific grant from funding agencies in the public, commercial, or not-for-profit sectors.

## Author Contribution statement

All the authors contributed to the conception or design of the work, the acquisition, analysis, and interpretation of data, drafting the work, and revising it critically for important intellectual content.

Each coauthor has seen and agrees with how his name is listed.

## Conflict of interest

The authors have no competing interest in publishing the present work.

## References

1. Early photocoagulation for diabetic retinopathy. ETDRS report number 9. Early Treatment Diabetic Retinopathy Study Research Group. *Ophthalmology*. 1991 May;98(5 Suppl):766–85
2. Sacconi R, Casaluci M, Borrelli E, Mulinacci G, Lamanna F, Gelormini F, *et al*. Multimodal Imaging Assessment of Vascular and Neurodegenerative Retinal Alterations in Type 1 Diabetic Patients without Fundoscopic Signs of Diabetic Retinopathy. *J Clin Med*. 2019 Sep 8;8(9):1409
3. Wilkinson CP, Ferris FL 3rd, Klein RE, Lee PP, Agardh CD, Davis M, *et al*; Global Diabetic Retinopathy Project Group. Proposed international clinical diabetic retinopathy and diabetic macular edema disease severity scales. *Ophthalmology*. 2003 Sep;110(9):1677–82
4. Solomon SD, Goldberg MF. ETDRS Grading of Diabetic Retinopathy: Still the Gold Standard? *Ophthalmic Res*. 2019;62(4):190–195
5. Classification of diabetic retinopathy from fluorescein angiograms. ETDRS report number 11. Early Treatment Diabetic Retinopathy Study Research Group. *Ophthalmology*. 1991 May;98(5 Suppl):807–22
6. Soares M, Neves C, Marques IP, Pires I, Schwartz C, Costa MÂ, *et al*. Comparison of diabetic retinopathy classification using fluorescein angiography and optical coherence tomography angiography. *Br J Ophthalmol*. 2017 Jan;101(1):62–68
7. Early Treatment Diabetic Retinopathy Study Research Group. Grading Diabetic Retinopathy from Stereoscopic Color Fundus Photographs - An Extension of the Modified Airlie House Classification: ETDRS Report Number 10. *Ophthalmology*. 2020 Apr;127(4S):S99-S119
8. Early Treatment Diabetic Retinopathy Study design and baseline patient characteristics. ETDRS report number 7. *Ophthalmology*. 1991 May;98(5 Suppl):741–56
9. Lee CS, Lee AY, Sim DA, Keane PA, Mehta H, Zarranz-Ventura J, *et al*. Reevaluating the definition of intraretinal microvascular abnormalities and neovascularization elsewhere in diabetic retinopathy using optical coherence tomography and fluorescein angiography. *Am J Ophthalmol*. 2015 Jan;159(1):101–10.e1
10. Schaal KB, Munk MR, Wyssmueller I, Berger LE, Zinkernagel MS, Wolf S. VASCULAR ABNORMALITIES IN DIABETIC RETINOPATHY ASSESSED WITH SWEEP-SOURCE OPTICAL

- COHERENCE TOMOGRAPHY ANGIOGRAPHY WIDEFIELD IMAGING. *Retina*. 2019 Jan;39(1):79–87
11. McHugh ML. Interrater reliability: the kappa statistic. *Biochem Med (Zagreb)*. 2012;22(3):276–82
12. Arya M, Sorour O, Chaudhri J, Alibhai Y, Waheed NK, Duker JS, Bauman CR. DISTINGUISHING INTRARETINAL MICROVASCULAR ABNORMALITIES FROM RETINAL NEOVASCULARIZATION USING OPTICAL COHERENCE TOMOGRAPHY ANGIOGRAPHY. *Retina*. 2020 Sep;40(9):1686–1695
13. Cui Y, Zhu Y, Wang JC, Lu Y, Zeng R, Katz R, *et al*. Comparison of widefield swept-source optical coherence tomography angiography with ultra-widefield colour fundus photography and fluorescein angiography for detection of lesions in diabetic retinopathy. *Br J Ophthalmol*. 2021 Apr;105(4):577–581
14. Wang M, Garg I, Miller JB. Wide Field Swept Source Optical Coherence Tomography Angiography for the Evaluation of Proliferative Diabetic Retinopathy and Associated Lesions: A Review. *Semin Ophthalmol*. 2021 May 19;36(4):162–167

## Tables

**Table 1** Demographic and clinical features of patients enrolled.

<b>Eyes (n)</b>	31
<b>Patients (n)</b>	21
<b>Age (mean ± SD, years-old)</b>	63 ± 15 years-old
<b>Sex (n, %)</b>	
<b>Male</b>	10 (48%)
<b>Female</b>	11 (52%)
<b>BCVA (IQR, LogMAR)</b>	0.30 (0.00-0.43)
<b>DR severity (n, %)</b>	
<b>Severe non proliferative DR</b>	2 (6.5%)
<b>Proliferative DR</b>	21 (67.7%)
<b>Severe proliferative DR</b>	8 (25.8%)

Abbreviation: n: number; SD: standard deviation; BCVA: best-corrected visual acuity; IQR: Inter-quartile range; DR: diabetic retinopathy; LogMAR: Logarithm of the Minimum Angle of Resolution.

**Table 2**

**2.A:** Inter-rater agreement between two readers by using WP-CFP, SD-OCTA, and WF-CFP and SD-OCTA through overlay software in detection of IRMA, NVE and ND.



**2.B:** Concordance values between WF-CFP, SD-OCTA, and WF-CFP and SD-OCTA through overlay software in detection of IRMA, NVE and ND.

<b>A Inter-rater agreement</b>		<b>IRMA</b>	<b>NVE</b>	<b>NVD</b>
WF-CFP		0.55	0.62	0.22
SD-OCTA		0.92	0.86	0.87
WF-CFP + SD-OCTA (overlay software)		0.89	0.93	0.94
<b>B Concordance</b>		<b>IRMA</b>	<b>NVE</b>	<b>NVD</b>
WF-CFP vs SD-OCTA		0.17	0.15	0.26
WF-CFP + SD-OCTA (overlay software)	vs WF-CFP	0.17	0.35	0.13
WF-CFP + SD-OCTA (overlay software)	vs SD-OCTA	0.57	0.59	0.74

Abbreviation: WF-CFP: wide-field color fundus photography; SD-OCTA: spectral-domain optical coherence tomography; IRMA: intraretinal microvascular abnormality; NVE: neovascularization of elsewhere; NVD: neovascularization of optic disc

## Figures

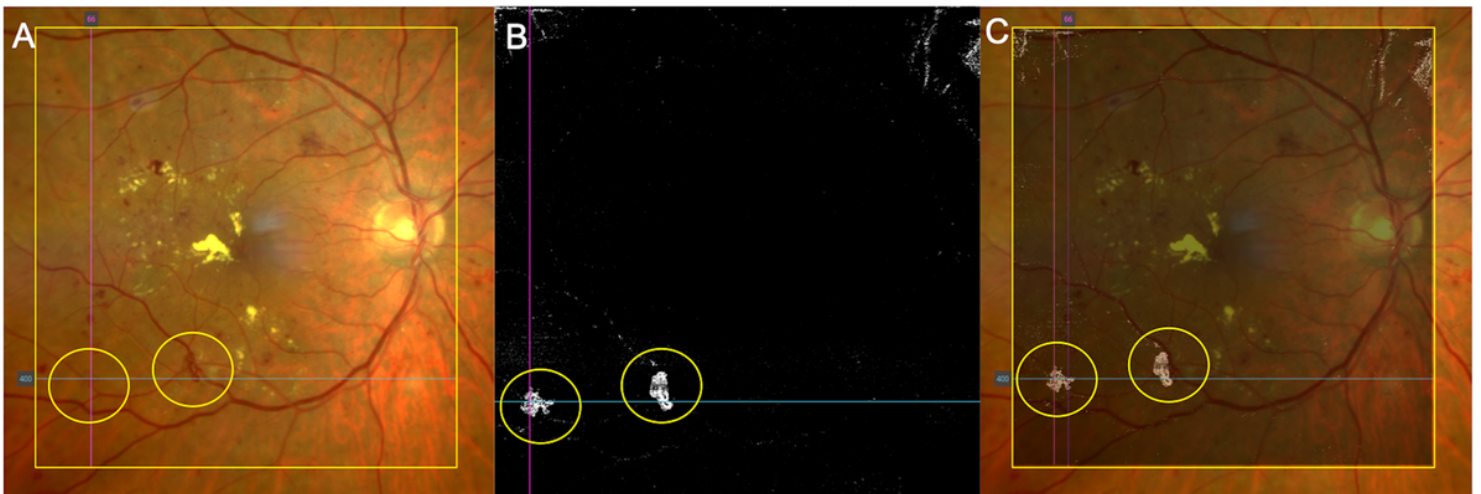


**Figure 1**

Detection of neovascularization elsewhere (NVE) (yellow circled areas) with three different techniques.

A: 12x12mm area of 90°Wide-Field Color Fundus Photography.

B: Vitreoretinal interface slab at Enface Wide-Field Spectral-Domain Optical Coherence Tomography Angiography (12x12mm scans)

C: Overlay between Color Fundus Photography and vitreoretinal interface slab at Enface Wide-Field Spectral-Domain Optical Coherence Tomography Angiography (12x12mm scans)

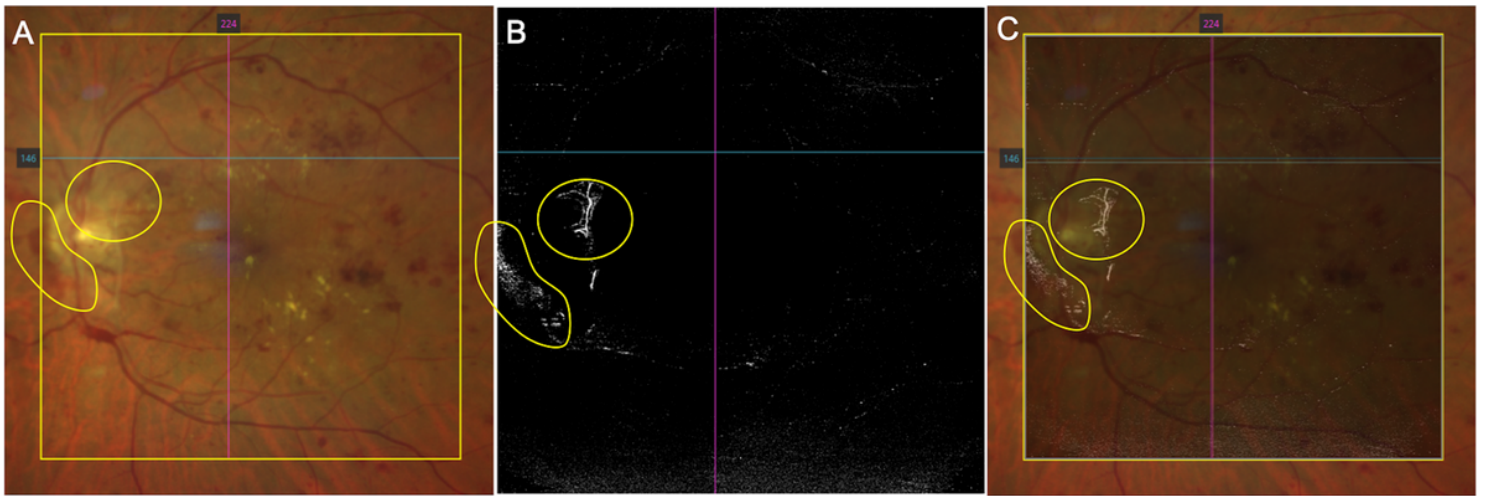


**Figure 2**

Detection of neovascularization of the optic disc (NVD) (yellow circled areas) with three different techniques.

A: 12x12mm area of 90° Wide-Field Color Fundus Photography.

B: Vitreoretinal interface slab at Enface Wide-Field Spectral-Domain Optical Coherence Tomography Angiography (12x12mm scans)

C: Overlay between Color Fundus Photography and vitreoretinal interface slab at Enface Wide-Field Spectral-Domain Optical Coherence Tomography Angiography (12x12mm scans)

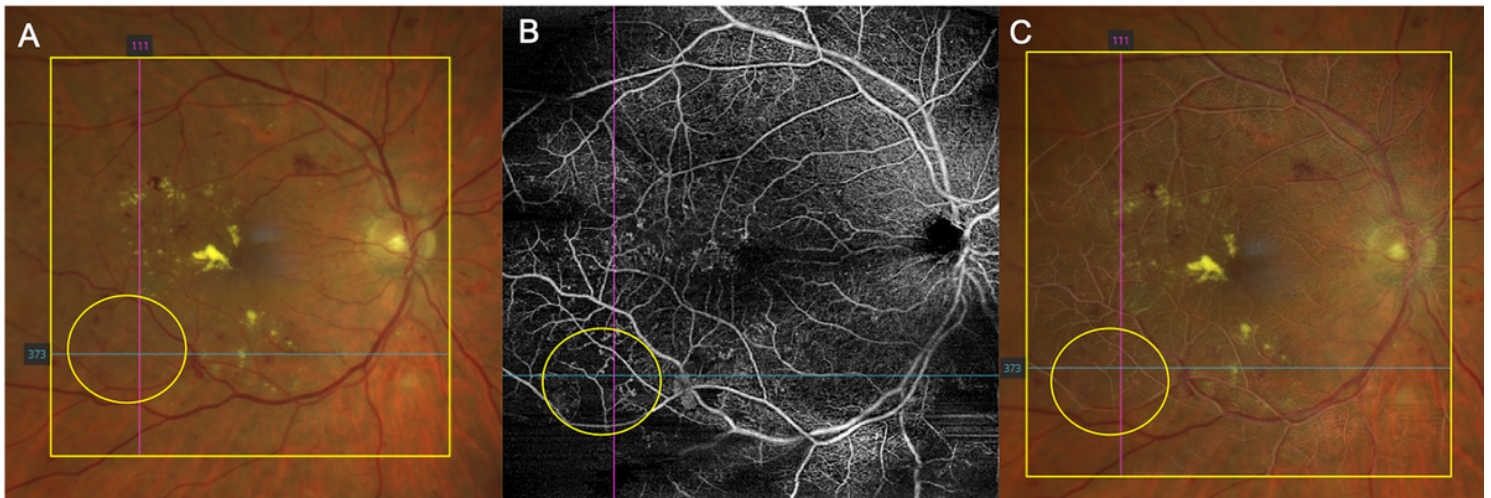


**Figure 3**

Detection of intraretinal microvascular abnormalities (IRMA) (yellow circled areas) with three different techniques.

A: 12x12mm area of 90°Wide-Field Color Fundus Photography.

B: Superficial Capillary Plexus (SCP) slab at Enface Wide-Field Spectral-Domain Optical Coherence Tomography Angiography (12x12mm scans)

C: Overlay between Color Fundus Photography and SCP slab at Enface Wide-Field Spectral-Domain Optical Coherence Tomography Angiography (12x12mm scans)